Extraction of Chromophoric Compounds from *Acer palmatum* Leaves: Optimization of Ternary Deep Eutectic Solvent-Assisted Extraction Process and Chromophore Stability Study

Jingyun Xie,[a] Yiqing Qi,[a,*] Yining Chen,[b] Xinye Lu,[c] and Zhiyi Wang, [d]

In this study, red leaves of *Acer palmatum* were used as raw material. A ternary deep eutectic solvent (DES) was used for auxiliary extraction, with the optimal extraction condition ranges determined by single-factor experiments. Then the process was optimized *via* response surface methodology (RSM). Using dye absorbance as the evaluation index, the acid-base stability, thermal stability, and light resistance of *Acer palmatum* extract were investigated, and the compounds in its dye were identified. The optimal extraction process was: a solid-to-liquid ratio of 1:15 (w:v), an extraction time of 112 min, a moisture content of 86%, and an extraction temperature of 42 °C. Fourier transform infrared spectroscopy analysis and stability tests were also conducted. Ternary DES extraction of Acer palmatum dye is a pollution-free, low-energy and sustainable process, providing practical reference for expanding the industrial application of natural dyes.

DOI: 10.15376/biores.21.3.7974-8000

Keywords: Acer palmatum dye; Ternary deep eutectic solvent; Natural dye extraction; Response surface optimization method; Stability

*Contact information: a: College of Furniture and Industrial Design, Nanjing Forestry University, Nanjing 210037, China; b: Collaborative Innovation Center for Efficient Processing and Utilization of Forest Resources of Jiangsu Province; c: College of Furniture and Industrial Design, Nanjing Forestry University, Nanjing 210037, China; d: College of Furniture and Industrial Design, Nanjing Forestry University, Nanjing 210037, China; *Corresponding author: yiqingqi@njfu.edu.cn*

INTRODUCTION

Research on natural dyes has garnered significant attention due to their environmental friendliness and sustainability. Among these, plant dyes have emerged as a focal point of study due to their widespread availability, structural diversity, and functional properties.

Acer palmatum Thunb. (red maple, or maple leaf) is a deciduous small tree belonging to the *Acer* genus of the Aceraceae family (Editorial Committee of Flora of China 2008). The red dyes in Japanese maple are primarily concentrated in anthocyanins, a class of water-soluble flavonoid compounds. As shown in Fig. 1(b), the basic structure of natural anthocyanin glycoside aglycones is 3,5,7-trihydroxy-2-phenylbenzopyran (Pang *et al*. 2000). This is composed of a C6-C3-C6 skeleton, with the anthocyanin moiety as its parent nucleus (An *et al*. 2012).

Acer palmatum dyes possess vibrant colors and excellent dyeing properties, offering potential applications in food, textiles, cosmetics, and other fields. In the food industry, *A. palmatum* dyes can serve as natural colorants. Compared to synthetic dyes, they offer advantages such as high safety and rich bioactivity. In the textile industry, maple dyes can be used for dyeing natural and synthetic fibers, offering natural color and environmental friendliness (Luo *et al*. 2018).

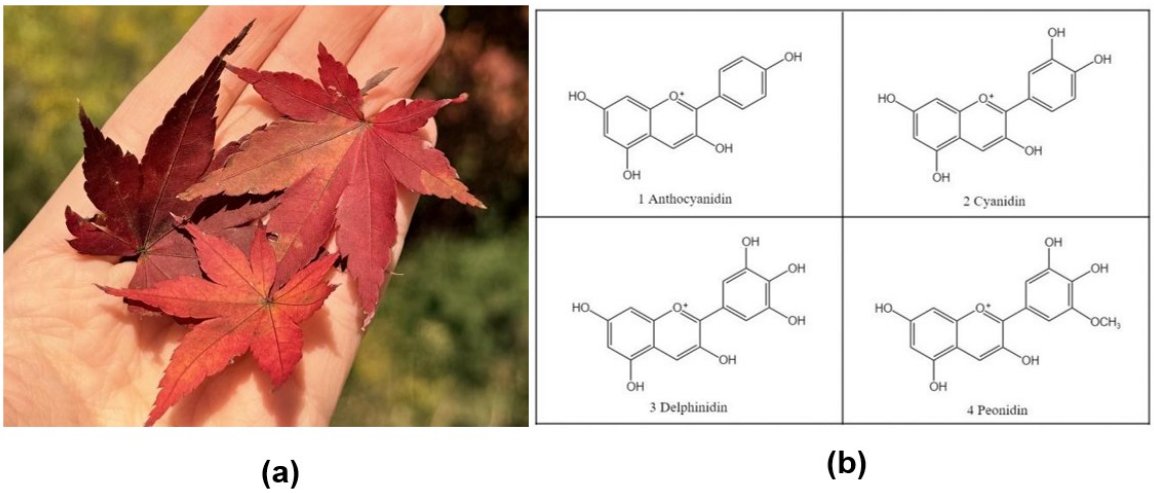

Fig. 1. (a) *Acer palmatum* leaf; (b) dye structure. Structural formula 1) Anthocyanin glycoside; 2) Cyanidin; 3) Delphinidin; 4) Paeoniflorin

Although natural dye research has achieved certain results, numerous challenges remain. Traditional methods for extracting *Acer palmatum* dye primarily employ conventional water extraction or solvent extraction, which are simple to operate, cost-effective, and use safe, non-toxic solvents. However, these traditional methods have drawbacks such as lengthy extraction times, low extraction efficiency, and high solvent consumption. Additionally, high temperatures during extraction may cause structural damage to the dye, affecting its stability and bioactivity, leading to degradation and loss of the dye (Abbott *et al*. 2004; Cai *et al*. 2015). Abbott *et al*. (2004) first proposed a novel green solvent formed by a hydrogen bond donor (HBD) and a hydrogen bond acceptor (HBA) through hydrogen bonding interactions, known as deep eutectic solvents (DESs). Their raw materials are often inexpensive and readily available, and the preparation process is simple. They are biodegradable and environmentally friendly, aligning with the principles of green chemistry, and they may become a focal point in ecological civilization construction (Gao *et al*. 2024). The hydrogen bonds formed between the hydroxyl or carboxyl groups in DESs and the extract not only increase the extraction rate of target compounds but also help maintain the stability of the extract (Yu *et al*. 2023). The application of DESs increases the solubility of flavonoid compounds, thereby improving the extraction efficiency of bioactive compounds in samples (Tang *et al*. 2015). Their strong designability allows for the adjustment of physical and chemical properties, such as polarity, viscosity, and melting point, by altering the types and ratios of hydrogen bond donors and acceptors, to accommodate the extraction requirements of different dyes. Chen *et al*. (2020) introduced a third component based on binary DESs, further optimizing the performance of DESs, achieving a lower eutectic point, and significantly improving reaction speed, effectively

increasing the yield of lignocellulosic biomass. Compared to binary DESs, ternary DESs (composed of three components) exhibit superior performance in dye extraction due to their unique physical and chemical properties, with notable improvements in solubility, selectivity, and stability (Jablonsky *et al*. 2019; Nie *et al.* 2023), offering a more optimal solution for the extraction of *Acer palmatum* dyes. This study will utilize ternary DESs to optimize the extraction of *Acer palmatum* dyes, thereby improving the extraction rate and quality of these dyes.

Since its introduction in the 1950s, Response Surface Methodology (RSM) has evolved into a mature method for experimental design and process optimization through long-term development. This method combines mathematical and statistical principles to analyze the influence of independent variables on response values and optimize complex technological processes. It has been widely applied in various fields such as chemistry, materials science, food science, and biotechnology (Cano-Lamadrid *et al*. 2023). Box-Behnken Design (BBD) is one of the commonly used response surface design methods, which utilizes quadratic polynomial regression equations to plot response surfaces and contour plots. In recent years, with the increasing demand for natural dyes in the food, pharmaceutical, and cosmetics industries, BBD has garnered significant attention in the optimization of their extraction processes. In this experiment, the prominent role of BBD is mainly reflected in the following aspects. The extraction efficiency of natural dyes is often influenced by a combination of factors, such as the type and concentration of extraction solvents, extraction temperature, extraction time, and the solid-to-liquid ratio (Sun *et al*. 2023). Compared to traditional single-factor optimization methods, which yield inaccurate results and have low experimental efficiency, BBD utilizes contour plots and response surface plots to systematically analyze the impact of multiple factors and their interactions on extraction efficiency, thereby identifying the optimal extraction conditions (Tian and Hu 2025). Furthermore, this design can avoid extreme level combinations and effectively estimate the coefficients in quadratic models, making it widely used by researchers in process optimization experiments (Diao *et al.* 2019; Qi *et al.* 2023). This method has been extensively applied in the optimization of extraction processes for plant natural dyes such as anthocyanins, chlorophyll, and carotenoids, enabling the acquisition of optimal solutions with fewer experimental trials, thereby significantly enhancing experimental and extraction efficiency. In the extraction of anthocyanins from rose eggplant, the yield and stability of anthocyanins have been significantly improved after optimization using response surface methodology. This method also facilitates refined control of the extraction process, enhancing resource utilization. Research on the extraction of procyanidins from tartary buckwheat shells indicates that process parameters optimized by response surface methodology can increase the extraction rate, enhance material utilization efficiency, and reduce waste (Sharma 2018).

Research on the extraction and application of *Acer palmatum* dye is relatively scarce, particularly in terms of its untapped potential in fields such as textile and wood dyeing. This study addressed the low extraction efficiency and poor stability of *A. palmatum* dye by using a deep eutectic solvent to extract the dye and investigate its properties. Based on the results of response surface experiments, the infrared spectra of *A. palmatum* dye were analyzed to explore the chemical composition of *A. palmatum* dye compounds. Single-factor experiments were conducted on the deep eutectic solvent extraction process for *A. palmatum* dyes to investigate the effects of feed-to-liquid ratio, extraction time, moisture content, and extraction temperature on the extraction process. Then, a Box-Behnken model was used to design a four-factor, three-level response surface

analysis experiment for coded analysis, establishing a quadratic multiple regression model to validate the effectiveness of the response surface method and optimize the optimal process conditions for deep eutectic solvent extraction of *Acer palmatum* dyes. The performance of different pH values, temperatures, and added reagents under UV irradiation was tested to provide scientific basis for the subsequent development and utilization of *Acer palmatum* dyes and to offer references for the development of the natural dye industry. Figure 2 shows the research flowchart.

EXPERIMENTAL

An overall representation of the experimental procedure is presented in Fig. 2.

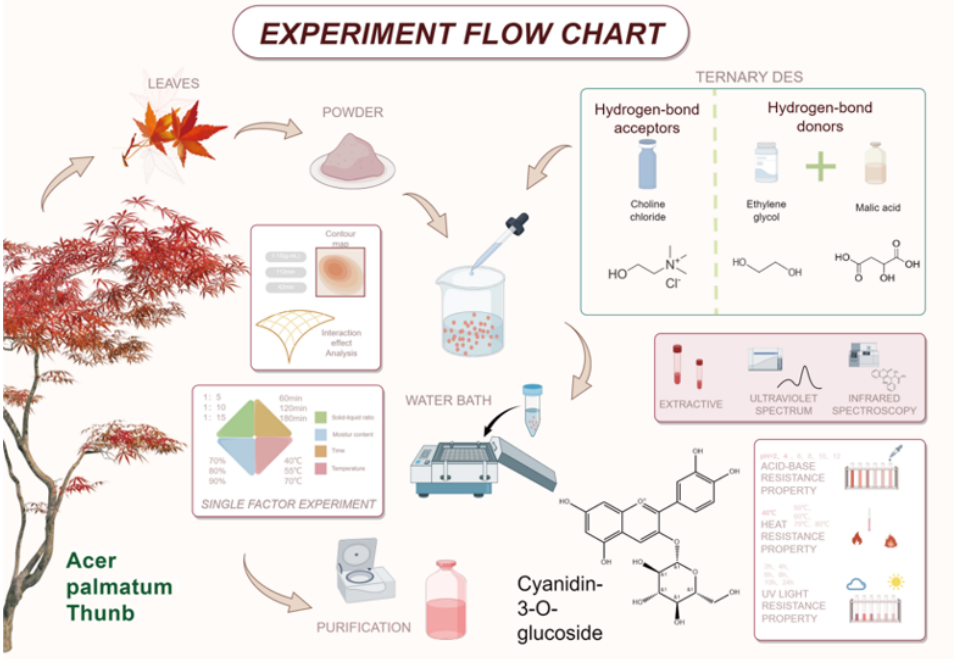

Fig. 2. Research flow chart

Materials

The raw materials and chemical reagents used in this study included: red leaves of *Acer palmatum* obtained during October to November from Nanjing, Jiangsu Province, China; ultrapure water made in the laboratory with analytical purity; cyanidin standard with purity ⩾98% (sourced from Nanjing Yuanzhi Biotechnology Co., Ltd.); ethylene glycol with purity ⩾99.5% (sourced from Sinopharm Chemical Reagent Co., Ltd.); malic acid with purity ⩾ 99.5% (sourced from Tianjin Kemio Chemical Reagent Co., Ltd.); hydrochloric acid with analytical purity; sodium hydroxide with purity ⩾96.0% (sourced from Nanjing Chemical Reagent Co., Ltd.); and tea polyphenols with purity 98% (sourced from Cool Chemical Science and Technology (Beijing) Co., Ltd.); CD_3OD, 99.0 atom % D.

Pretreatment of Dye Raw Materials

First, the *Acer palmatum* leaves were washed with water and dried. An appropriate amount of dried *A. palmatum* was cleaned to remove any surface impurities, ground into

powder, and stored powder in an airtight container. An appropriate amount of 1 g of *A. palmatum* powder was mixed with pure water. To prevent dye degradation due to high temperature or prolonged exposure, the solution was extracted in a water bath at 55 °C for 90 min.

Characterization

Ultraviolet-visible light analysis

Using an appropriate amount of *Acer palmatum* powder, a solution was prepared with pure water. A U-3900 ultraviolet spectrophotometer was used to determine the ultraviolet-visible absorption spectrum curve of the sample in the range of 300 to 700 nm. The maximum absorption wavelength was determined, and the dye content in the solution was characterized by the absorbance at the maximum absorption wavelength.

Fourier transform infrared spectroscopy

A VERTEX 80V Fourier transform infrared spectrometer (Bruker, Karlsruhe, Germany) was used. Before testing, the *Acer palmatum* dye samples were thoroughly ground with potassium bromide and pressed into pellets. The samples were kept dry and clean to avoid the influence of moisture on the data. Scanning was performed using the Smarti TR diamond ATR mode. The window background was scanned and measured to remove interference, with 16 scans conducted. The sample was then placed, and 16 scans were performed within the wave number range of 4000 to 500 cm^{-1}.

Dyes Extraction Experiment

Preparation of ternary low eutectic solvents

Choline chloride acts as a hydrogen bond acceptor (HBA), with its chloride ions (Cl-) bonding to the -OH groups of ethylene glycol, disrupting the intermolecular hydrogen bonds within ethylene glycol and lowering the melting point of the system. Cl- also bonds with the hydroxy groups of malic acid, forming a multi-hydrogen bond network that enhances the solvent's ability to dissolve target substances. The synergistic hydrogen bonding effects of the three components significantly lower the melting point of the mixed system, enabling DESs to remain liquid at room temperature for convenient handling. Choline chloride, ethylene glycol, and malic acid are industrially produced on a large scale, with widespread availability and controllable costs. Among these, choline chloride and malic acid are biodegradable by microorganisms, while ethylene glycol exhibits extremely low volatility in DESs due to hydrogen bonding fixation. Therefore, choline chloride, ethylene glycol, and malic acid were mixed in a molar ratio of 1:3:1 to prepare the solvent. The prepared solvent was then heated in a 50 °C constant-temperature water bath for 30 min to obtain a clear and transparent deep eutectic solvent, which is then removed and cooled to room temperature for later use.

Single-factor experimental design

The single factor test was carried out by selecting four factors: material-liquid ratio, extraction time, moisture content and temperature. Since the absorbance of dye content in natural dyes is more intuitive, the absorbance of *A. palmatum* dye was used as the evaluation index to determine the optimal range of the four factors. The levels of each factor in the single experiments are shown in Table 1.

Table 1. Single-factor Experiment: Factors and Levels

	Feed-to-Liquid Ratio (w:v)	Time (min)	Moisture Content (%)	Temperature (°C)
1	1:5	30	40	10
2	1:10	60	50	25
3	1:15	90	60	40
4	1:20	120	70	55
5	1:25	150	80	70
6	1:30	180	90	85

Feed-to-liquid ratio

The solvent configured in the above text is used as the research object to investigate the effect of the feedstock-to-solvent ratio on dye extraction efficiency. Single-factor experiments were conducted with solid-to-liquid ratios of 1:5, 1:10, 1:15, 1:20, 1:25, and 1:30 under the same extraction conditions: extraction temperature of 50 °C, extraction time of 120 min in a water bath, and moisture content of 60%. After the reaction was complete, the crude extract was filtered and vacuum-filtered, and the absorbance was measured.

Extraction time

Extraction was conducted under the same conditions: a solid-to-liquid ratio of 1:10, an extraction temperature of 50 °C, and a moisture content of 60%, with extraction times of 30, 60, 90, 120, 150, or 180 min as single variables. After the reaction was complete, the crude extract was filtered and vacuum-filtered, and the absorbance was measured.

Moisture content

Distilled water was added to the low eutectic solvent in proportions to achieve water content levels of 40, 50, 60, 70, 80, or 90%. Extraction was then carried out under the same conditions: a feed-to-solvent ratio of 1:10, an extraction temperature of 50 °C, and a duration of 120 min. After the reaction was complete, the crude extract was filtered and vacuum filtered, and its absorbance was measured.

Extraction temperature

Experiments were conducted using extraction temperatures of 10, 25, 40, 55, 70, or 85 °C as single variables. Under the same extraction conditions, the solid-liquid ratio was 1:10, the extraction temperature was 50 °C, and the extraction time was 120 min. After the reaction was complete, the crude extract was filtered and vacuum-filtered, and the absorbance was measured.

Optimization of extraction conditions

Based on the analysis of output values and input parameters and their interactions, response surface methodology (RSM) can quickly and accurately obtain the optimal response value through reasonable selection of test points and iterative strategies (Yu *et al*. 2023). RSM was used to extract *Acer palmatum* dye with a low eutectic solvent. The aim was to use RSM to optimize the extraction of *A. palmatum* dye with a low eutectic solvent to obtain the optimal process conditions, improve extraction efficiency, and avoid the use of harmful chemicals.

The Design Expert 11 software (Stat-Ease, 11, Minneapolis, MN, USA) was used to develop a test plan based on the Box-Behnken model. Based on the results of the single-factor experiment, the experimental factors were selected as liquid-to-solid ratio (A), extraction time (B), moisture content (C), and extraction temperature (D), with absorbance as the response

value. A four-factor response surface analysis experiment was designed for coded analysis, with the central experiment repeated three times. The Box-Behnken test factor level design is shown in Table 2.

Table 2. Box-Behnken Test Factor Level Design

Horizontal	Factors			
	A Feed-to-Liquid Ratio (w:v)	B Time (min)	C Moisture Content (%)	D Extraction Temperature (°C)
-1	1:5	60	70	40
0	1:10	120	80	55
1	1:15	180	90	70

Dye Stability Study

The *Acer palmatum* dye solution was extracted. The acid-base stability, thermal stability, and UV light stability of the dye solution were examined to provide a reference for the subsequent dyeing process.

pH value

To investigate the effect of acidity and alkalinity on the stability of the *Acer palmatum* dye solution, six 20 mL samples of the *A. palmatum* dye solution were taken. The pH of the dye solution was adjusted to 2, 4, 6, 8, 10, and 12 using sodium hydroxide and dilute hydrochloric acid, respectively. The solutions were incubated at 25 °C in a water bath for 2 h. Changes in the dye solution were observed. Next, 0.5 mL of the tested *A. palmatum* dye solution was diluted with 25 mL of pure water, and the ultraviolet-visible absorption spectrum curve was measured to compare the effects of different pH levels on the stability of the dye.

Temperature

To investigate the effect of temperature on the stability of A. palmatum dye solutions, five 20 mL samples of A. palmatum dye solutions were taken and incubated in water baths at temperatures of 40, 50, 60, 70, or 80 °C for 2 h. The changes in the dye solutions were observed, and then 0.5 mL of the tested A. palmatum dye solution was diluted with 25 mL of pure water, and the ultraviolet-visible absorption spectrum curve was tested to compare the effects of different temperatures on the stability of the dye solutions.

Sun resistance

To investigate the effect of ultraviolet (UV) light exposure on the stability of *A. palmatum* dye solutions and whether the addition of antioxidant tea polyphenols affects the dye's light stability, 24 samples of 20 mL *A. palmatum* dye solutions of the same concentration were divided into 4 groups, with 6 samples per group. Different groups were treated with pure water, DES, 0.48 g tea polyphenols, and 0.06 g tea polyphenols, respectively. Each group was exposed to a 30 W UV lamp for 2, 4, 6, 8, 10, or 24 h, and changes in the dye solution were observed. After testing, 0.5 mL of the *A. palmatum* dye solution was diluted with 25 mL of pure water, and the UV-visible absorption spectrum curve was tested and plotted to compare the effects of different UV light exposure durations on the stability of the dye solution.

RESULTS AND DISCUSSION

Physical and Chemical Evaluation

Ultraviolet-visible absorption spectrum

According to Fig. 3, the ultraviolet-visible absorbance spectrum of *Acer palmatum* dye at wavelengths of 400 to 700 nm showed that the maximum absorbance wavelength was 514 nm.

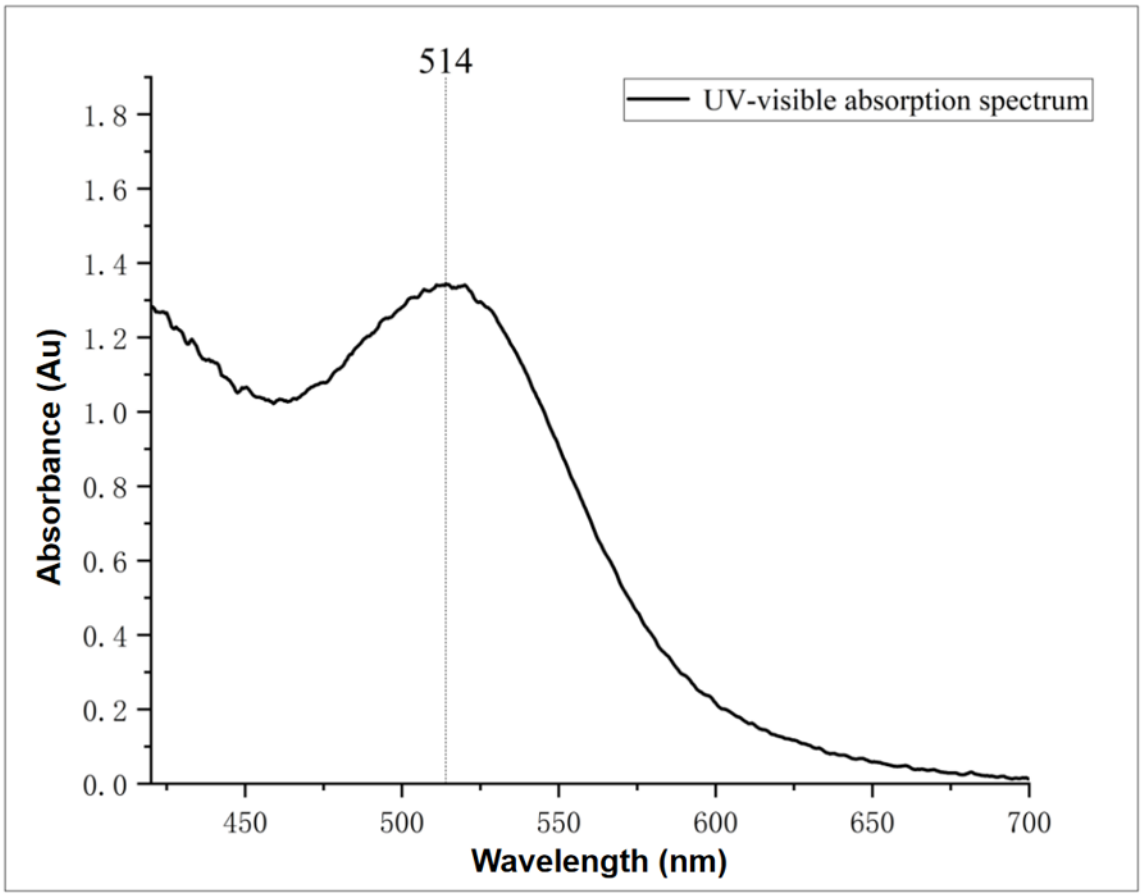

Fig. 3. Full-waveband absorption spectrum of *Acer palmatum* dye in ultraviolet-visible light

Fourier transform infrared spectroscopy

Figure 4 shows the infrared spectrum of *A. palmatum* dye. As can be seen from the figure, the main peaks of the infrared scan of *A. palmatum* dye were largely consistent with those of the standard sample of cyanidin-3-O-glucoside, indicating that the functional groups of the main components in *A. palmatum* dye were consistent with those of cyanidin-3-O-glucoside. This spectrum was primarily characterized by three segments: 4000 to 2800 cm^{-1}; 1800 to 900 cm^{-1}; and 900 to 500 cm^{-1}. The approximate wavenumber 3405 cm^{-1} represents the stretching vibration of O-H. The spectral information was rich and strong in the wave number range of 1730 to 1410 cm^{-1}, which is primarily the absorbance region for C=O stretching vibrations. C=O is abundantly present in flavonoids and alkaloids. The wavenumber 1728.7 cm^{-1} corresponds to the C=O stretching vibration of the aldehyde group; 1638.4 cm^{-1} corresponds to the aromatic ring C=C stretching vibration; 1520.1 cm^{-}

[1] is the skeletal vibration of the aromatic ring C=C, one of the characteristic absorption peaks of flavonoids, indicating the conjugated structure of the benzene ring; 1444.2 cm^{-1} and 1413.7 cm^{-1} are the symmetric stretching vibrations of the hydroxide ion (COO-); 1076.1 cm^{-1} is the C-O stretching vibration; 875.6 and 857.9 cm^{-1} correspond to the out-of-plane bending vibrations of C-H bonds in the aromatic ring with para-substituted groups; at 624.4 cm^{-1}, there was an out-of-plane bending vibration of C-H bonds in the aromatic ring. The above analysis, as shown in Table 3, provides information on the chemical composition of the *A. palmatum* dye.

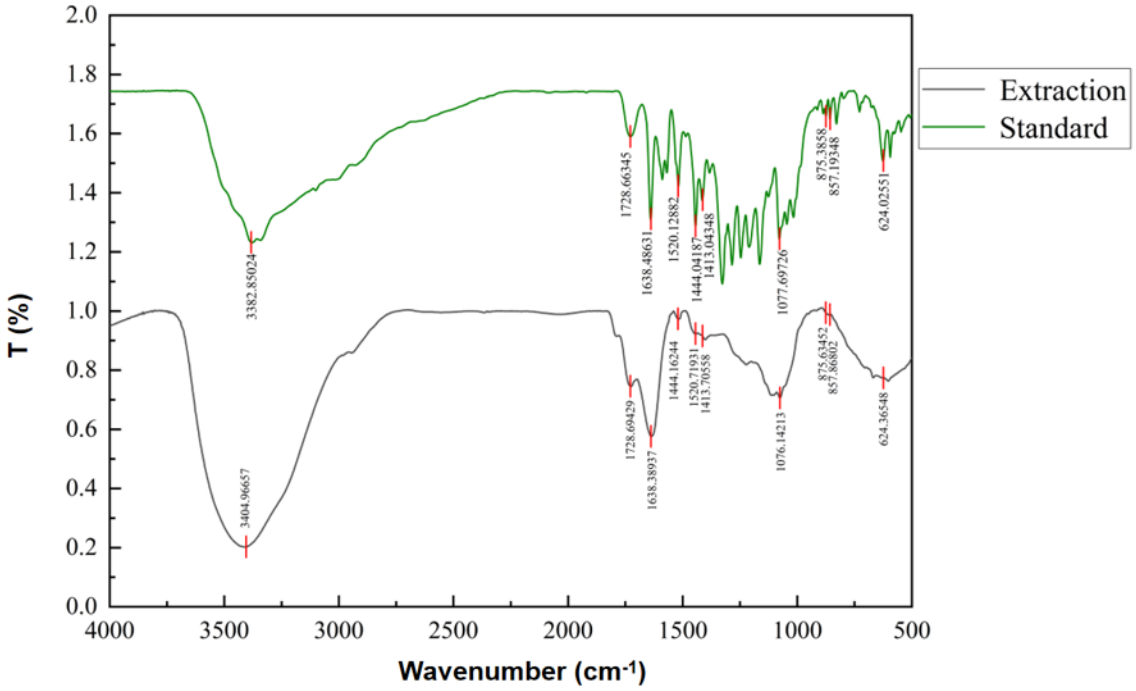

Fig. 4. Infrared spectral analysis of *Acer palmatum* dye

[4]H NMR analysis

1H NMR spectra were recorded on a Bruker DPX 400 MHz spectrometer in CD3OD. Chemical shifts were reported in ppm with the internal TMS signal at 0.0 ppm as a standard. The spectra are interpreted as: s, singlet; bs, broad singlet; d, doublet; t, triplet; q, quartet; m, multiplet; dd, double doublet; ddd, double double doublet; dt, double triplet; ddt, double double triplet; tt, triple triplet, td, triple doublet; coupling constant(s) J are reported in Hz and relative integrations are reported.

Table 3. FTIR Spectral Characteristics and Peak Properties of *Acer palmatum* Dye

Peak (cm^{-1})	Group description
1728.7	O-H extensible vibration
1638.4	Aromatic ring C=C stretching vibration
1520.1	Aromatic ring C=C backbone vibration
1444.2	Symmetrical expansion and contraction movement of hydroxylic acid ions (COO^-)
1413.7	Symmetrical expansion and contraction movement of hydroxylic acid ions (COO^-)
1076.1	C-O extensional vibration
875.6	C-H out-of-plane bending vibration
857.9	C-H out-of-plane bending vibration
624.4	C-H out-of-plane bending vibration

NMR Analysis

Standard (Cyanidin-3-O-glucoside, C3G):

^{1}H NMR (400 MHz, CD_3OD) δ 9.02 (s, 1H, OH), 8.28–8.25 (m, 1H, H-6′), 8.03 (d, J = 4.0 Hz, 1H, H-2′), 7.01 (d, J = 8.0 Hz, 1H, H-5′), 6.89 (d, J = 4.2 Hz, 1H), 6.65 (s, 1H), 5.31 (d, J = 8.2 Hz, 1H, anomeric H), 3.94–2.77 (m, sugar protons). The low-field singlet at δ 9.02 was assigned to a hydrogen-bonded hydroxyl proton. The aromatic ABX system (δ 8.03, 7.01, 8.28–8.25) confirmed the 3′,4′-dihydroxy substitution on ring B. The anomeric proton at δ 5.31 (d, J = 8.2 Hz) indicated a β-configuration. Thus, the standard was identified as cyanidin-3-O-glucoside.

Sample (Acer palmatum dye):

The sample exhibited sugar region signals (δ 3.0–5.5 ppm) highly consistent with the C3G standard, including the anomeric proton at δ ~5.3 ppm and glucose ring proton multiplets at δ 3.0 to 4.0 ppm, confirming the presence of anthocyanin glucosides. However, the aromatic region (δ 6.5 to 9.0 ppm) did not perfectly match the standard . Together with the overlapping sugar signals, this indicates that the sample is not pure cyanidin-3-O-glucoside, but a mixture of various anthocyanin-3-glucoside derivatives.

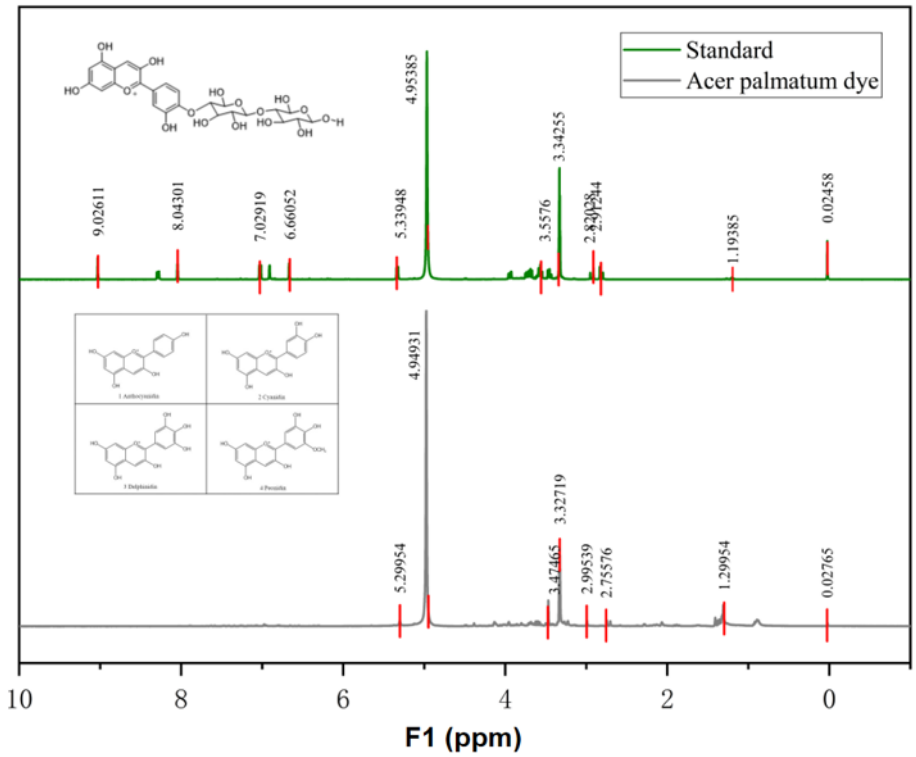

Fig. 5. ^{1}H NMR spectra of cyanidin-3-O-glucoside and *Acer palmatum* anthocyanin sample

Results of Single-Factor Experimental Design for Malic Acid

Material-to-liquid ratio

The solid-to-liquid ratio refers to the ratio of the mass of *Acer palmatum* leaf powder (g) to the volume of extraction solvent (mL), reflecting the balance between solid–liquid mass transfer kinetics and the effective concentration of the extraction solvent. By setting a series of gradient solid-to-liquid ratios, the optimal condition that ensures both high extraction efficiency and reasonable solvent consumption can be determined, thereby providing an appropriate range of factor levels for the subsequent response surface optimization experiment.

Under fixed extraction time and temperature conditions, the effect of the solid-to-liquid ratio on extraction efficiency can be divided into two stages. When the solid-to-liquid ratio is relatively high, that is, when the amount of solvent is relatively low, solid–liquid contact is insufficient, and the migration of dyes from the solid phase to the liquid phase is restricted, resulting in a low extraction yield. As the solid-to-liquid ratio gradually decreases, namely as the solvent volume increases, the solid–liquid mass transfer efficiency is significantly improved, leading to an increase in extraction yield. However, once the solid-to-liquid ratio falls below a certain critical value, further increasing the solvent volume may instead produce adverse effects. On the one hand, the effective concentration of the hydrogen bond donor, malic acid, in the DES is excessively diluted, weakening its stabilizing effect on dye molecules and its extraction capacity. On the other hand, excessive solvent causes the extracted dye molecules to become overly dispersed in the liquid phase, which may increase their sensitivity to environmental factors such as oxygen and light, and

may even lead to partial dye degradation. The combined effects of these factors ultimately result in a decrease in extraction yield.

Figure 6a shows the effect of the solid-to-liquid ratio between *A. palmatum* leaf powder and the ternary DES on the absorbance of the dye extract. The results indicate that the absorbance reached its maximum value at a solid-to-liquid ratio of 1:5 (w/v), suggesting that the dye extraction efficiency was optimal under this condition. As the solid-to-liquid ratio was further decreased, for example below 1:5, the absorbance showed a downward trend, which is consistent with the above analysis. Therefore, solid-to-liquid ratios of 1:5, 1:10, and 1:15 were selected as the three levels for further investigation in the subsequent response surface optimization experiment.

Extraction time

During the extraction process, time directly affects changes in intracellular temperature, the extent of cell wall rupture, and the solubility of compounds. Figure 6b shows the effect of extraction time on dye absorbance. The absorbance of the *A. palmatum* dye extract was influenced by extraction time. When the extraction time was less than 60 min, the *A. palmatum* and deep eutectic solvent were not fully mixed, resulting in incomplete cell wall rupture, decreased dye extraction efficiency, and low dye absorbance. As time increased, the dye solution's absorbance increases, reaching a peak at 60 min of extraction time; however, as extraction time continues to increase beyond 60 min, polyphenolic compounds may be degraded or converted, leading to reduced dye content and a decreasing trend in dye absorbance (Nekkaa *et al*. 2023). Additionally, prolonged extraction increases energy consumption and costs. Therefore, considering both extraction efficiency and cost, 60 min was determined as the optimal extraction time. In subsequent response surface optimization experiments, 60, 120, and 180 min were selected as the three levels of response surface optimization factors to further optimize the extraction process parameters.

Moisture content

Figure 6c shows the effect of moisture content on dye absorbance. The absorbance of *A. palmatum* dye extract was influenced by moisture content. When the moisture content ranged from 40% to 80%, the absorbance of *A. palmatum* dye continued to increase. An increase in moisture content causes water molecules to interact with the solvent through hydrogen bonds, reducing the viscosity of the DESs and facilitating dye dissolution, thereby improving extraction efficiency (Jin *et al*. 2025). When the moisture content was 40%, the absorbance is lowest, as the low eutectic solvent contained less water, and the high viscosity hindered mass transfer and diffusion of the compounds, resulting in a lower extraction rate (Shang *et al*. 2019). When the water content was 80%, the absorbance of *A. palmatum* dye reached its maximum value; when the water content exceeded 80%, the high water content affected hydrogen bonding interactions, limiting the interaction between DESs and the target components (García *et al*. 2016), thereby affecting the extraction rate of *Cinnamomum camphora* fruit dye, and the absorbance decreases instead. Therefore, 80% was set as the optimal water content. In response surface optimization experiments, water content levels of 70, 80, and 90% were selected as the three levels for response surface optimization factors.

Temperature

Figure 6d shows the effect of extraction temperature on dye absorbance, with the absorbance of *Acer palmatum* dye extracts being influenced by extraction conditions. At lower extraction temperatures, the dye was not fully dissolved in the solvent, resulting in lower extraction rates. As temperature increases, solution viscosity and surface tension decrease (Nekkaa *et al.* 2023), which accelerates the penetration of DESs into *Acer palmatum* cells (Bişgin *et al.* 2025). This facilitated the release of phenolic compounds and increasing absorbance, reaching a peak at an extraction temperature of 55 ℃. Higher temperature reduced the hydrogel bond stability. Meanwhile, dye absorbance was reduced owing to the hydrogen bond destructions and reconstructions. Regarding the peak shift observed in Fig. 6d, as the extraction temperature increased, the absorption maximum of the dye extract exhibited a notable shift towards shorter wavelengths (hypsochromic shift), with more pronounced changes occurring at higher temperatures. This phenomenon may be attributed to temperature-induced disruption of the hydrogen bonding network between the dye molecules and the DES components, which alters the solvation state and electronic transition energy of the dye. Additionally, elevated temperatures may promote the conversion of anthocyanins among their various equilibrium forms, such as from the flavylium cation to the quinonoidal base or chalcone, each of which displays a distinct absorbance maximum. The combined effects of these factors likely account for the observed spectral behavior. Therefore, 55 ℃ was selected as the optimal extraction temperature. In response surface optimization experiments, 40, 55, and 70 ℃ were selected as the three levels for the subsequent Box-Behnken design to identify the optimal extraction temperature.

Single-factor experiment results

Figure 6 presents the results of single-factor experiments for the four extraction parameters: solid-to-liquid ratio, extraction time, moisture content, and extraction temperature. The optimal conditions identified from these experiments were a solid-to-liquid ratio of 1:5 (w/v), an extraction time of 60 min, a moisture content of 80%, and an extraction temperature of 55 °C. These four optimal values were then used as the center points for selecting the three-level factor ranges in the Box-Behnken response surface design.

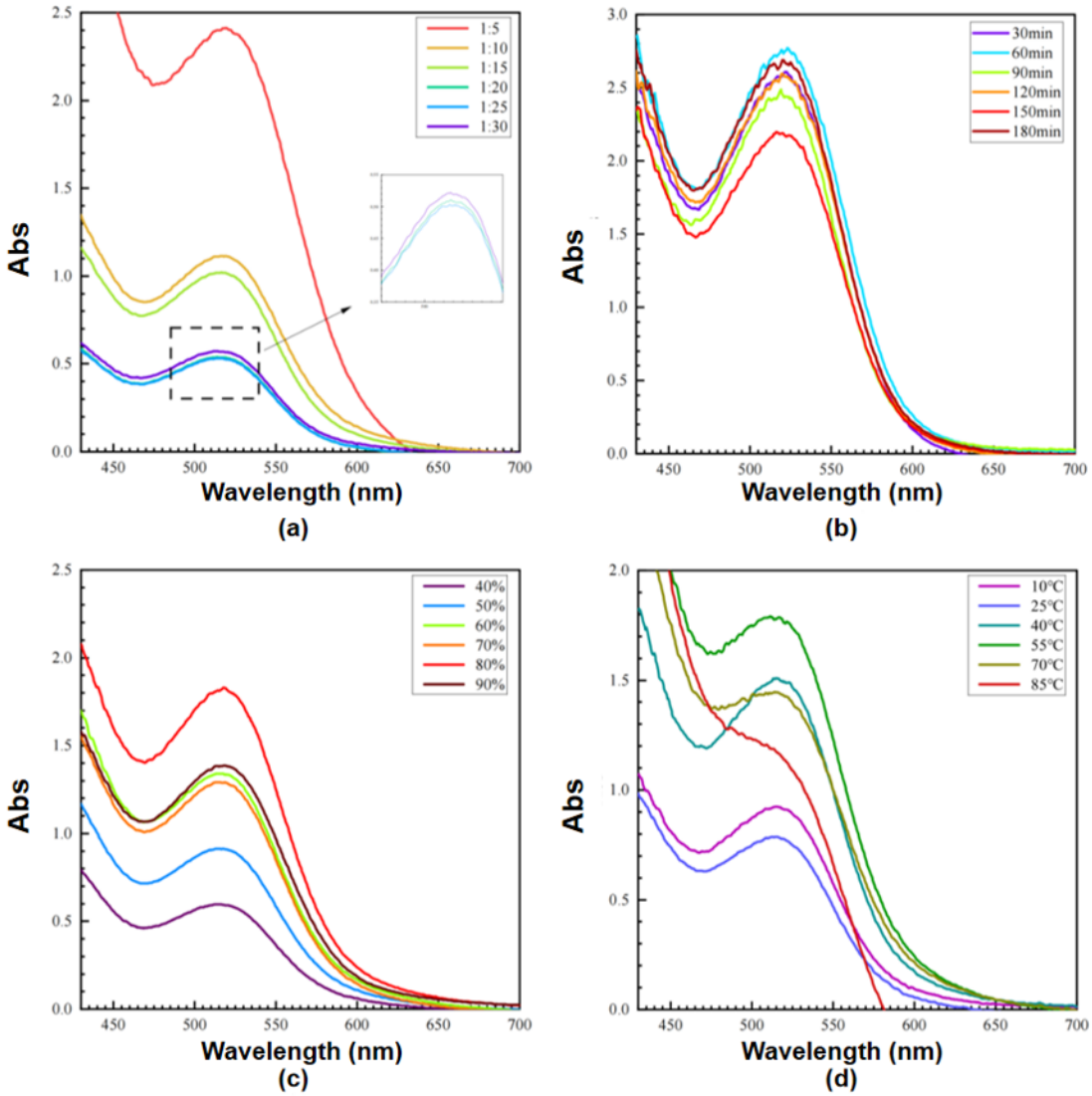

Fig. 6. (a) Effect of feedstock ratio on dye absorbance; (b) effect of extraction time on dye absorbance; (c) effect of moisture content on dye absorbance; (d) effect of extraction temperature on dye absorbance

Optimization of Extraction Conditions

Box-Behnken design and analysis

Based on the conclusions of the single-factor experiment, with absorbance as the response value, the experimental factors were selected as liquid-to-solid ratio (A), extraction time (B), moisture content (C), and extraction temperature (D). Using Design Expert 11 software and the Box-Behnken model, a four-factor, three-level response surface design experiment plan was formulated. The response surface experiment plan and results are shown in Table 4.

Fitting of second-order polynomial equations

Based on the results of the response surface experiment shown in Table 4, a regression model was established for the process parameters of *Acer palmatum* dye extraction. The quadratic polynomial regression equation for the response values of the

independent variables A (liquid-to-solid ratio), B (time), C (moisture content), and D (temperature) based on the absorbance of the *Acer palmatum* dye extract is as follows,

Absorbance of Phellodendron dye (R)=0.4862-0.0292A-0.0859B+0.0804C-0.0278D+0.4575AB+0.0387AC-0.1593AD+0.029BC-0.0208BD-0.18CD + 0.5794A2 + 0.3547B2 + 0.2632C2 + 0.6514D2

where A (material-liquid ratio), B (time), C (moisture content), and D (temperature) are test (input) variables.

Table 4. Box-Behnken Test Plan and Results

Sample	A Feed-to-Liquid Ratio (w:v)	B Time (min)	C Moisture Content (%)	D Temperature (°C)	R Absorbance of *Acer palmatum* dye (Abs)
1	0	1	0	1	1.336
2	0	0	0	0	0.47
3	-1	1	0	0	0.98
4	1	0	0	-1	1.94
5	1	1	0	0	1.79
6	0	1	0	-1	1.415
7	0	0	1	-1	1.655
8	0	0	0	0	0.55
9	0	-1	1	0	1.321
10	-1	0	0	-1	1.672
11	1	0	0	1	1.501
12	-1	-1	0	0	1.96
13	1	0	-1	0	1.168
14	-1	0	1	0	1.36
15	0	1	-1	0	0.887
16	0	0	0	0	0.451
17	0	-1	0	1	1.559
18	-1	0	-1	0	1.265
19	0	1	1	0	1.11
20	0	-1	-1	0	1.214
21	1	0	1	0	1.418
22	0	0	-1	1	1.501
23	0	0	1	1	1.286
24	0	-1	0	-1	1.555
25	1	-1	0	0	0.94
26	0	0	0	0	0.43
27	0	0	0	0	0.53
28	0	0	-1	-1	1.15
29	-1	0	0	1	1.87

Interaction effect analysis

The slope of the response surface reflects the sensitivity of the response of *Acer palmatum* dye to changes in processing conditions. A steep slope indicates that the response value is sensitive to changes in processing conditions; a gentle slope indicates that the response value is insensitive to changes in processing conditions. In the contour plot, an elliptical shape indicates that the interaction between the two factors is significant, while a circular shape indicates that the interaction between the two factors is not

significant. From the changes in the slope of the response surface shown in Fig. 7, the interaction between the factors affecting the absorbance of *A. palmatum* dye can be observed. Analysis of the three-dimensional response surface plot and two-dimensional contour plot shows that when any one of the factors (liquid-to-solid ratio, extraction time, moisture content, or extraction temperature) is at the 0 level, the interaction of the remaining three factors affects the absorbance of the *A. palmatum* dye solution. The surface formed by A and B is relatively steep, indicating that the interaction between the two has the most significant effect on the absorbance of the *A. palmatum* dye. As extraction time, solid-liquid ratio, time, moisture content, and extraction temperature increased, the absorbance of the *A. palmatum* dye also increased. However, when the solid-liquid ratio, extraction time, moisture content, and extraction temperature reached a certain level, the absorbance of the *A. palmatum* dye showed a decreasing trend. The experimental results are consistent with the variance analysis of the regression model. Table 5 presents the results of the variance analysis of the regression model.

Table 5. Analysis of Variance of Regression Models

Sources of variance	Sum of squares	degree of freedom	Mean square	F-value	P-value	Significance
Model	5.61	14	0.4004	102.67	< 0.0001	significant
A-Feed-to-liquid ratio	0.0102	1	0.0102	2.62	0.128	
B-Time	0.0886	1	0.0886	22.71	0.0003	
C-moisture content	0.0776	1	0.0776	19.9	0.0005	
D-Temperature	0.0093	1	0.0093	2.38	0.1449	
AB	0.8372	1	0.8372	214.68	< 0.0001	
AC	0.006	1	0.006	1.54	0.235	
AD	0.1014	1	0.1014	26.01	0.0002	
BC	0.0034	1	0.0034	0.8626	0.3688	
BD	0.0017	1	0.0017	0.4416	0.5171	
CD	0.1296	1	0.1296	33.23	< 0.0001	
A^2	2.18	1	2.18	558.28	< 0.0001	
B^2	0.8162	1	0.8162	209.3	< 0.0001	
C^2	0.4495	1	0.4495	115.25	< 0.0001	
D^2	2.75	1	2.75	705.67	< 0.0001	
Residual	0.0546	14	0.0039	——	——	
Lack of Fit	0.0439	10	0.0044	1.65	0.3325	not significant
Pure Error	0.0106	4	0.0027	——	——	
Cor Total	5.66	28	——	——	——	
R^2 0.9904						

Note: * indicates p < 0.05, significant difference; ** indicates p < 0.01, extremely significant difference.

Using the absorbance of *A. palmatum* dye as the evaluation criterion, variance analysis was performed on the model, and the significance of the model coefficients was tested. From the table, it can be concluded that the model was highly significant, with $p<0.01$, ($p <0.05$ $p<0.01$), and the F-value for the lack-of-fit term is 1.65, indicating that the lack of fit was not significantly different from the pure error. The coefficient of determination for the regression model was 0.9904, indicating that the model can explain 99.04% of the variance. The model had a good fit, and the experimental error was within a

reasonable range. Optimizing the extraction process of *A. palmatum* dye using this model can yield good results. The linear terms A, B, C, and D in the model were significant ($p<0.05$, $p<0.01$). Using the F value of the linear terms in the quadratic regression equation as a basis for comparing the effects of each parameter on the absorbance of *A. palmatum* bark dye, it can be seen that the magnitude of the effects of the four factors on the absorbance of *A. palmatum* bark dye was as follows: B>C>A>D, *i.e.*, extraction time > moisture content > liquid-to-solid ratio > extraction temperature. The magnitude of the interaction effects was AB>CD>AD>AC>BC>BD.

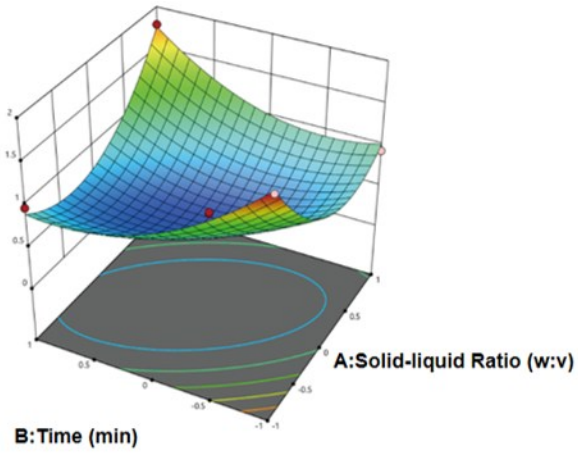

(a)

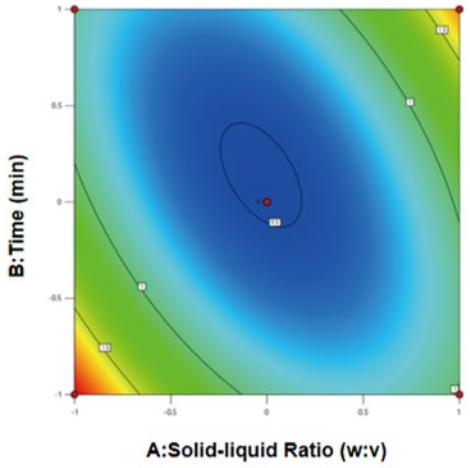

(b)

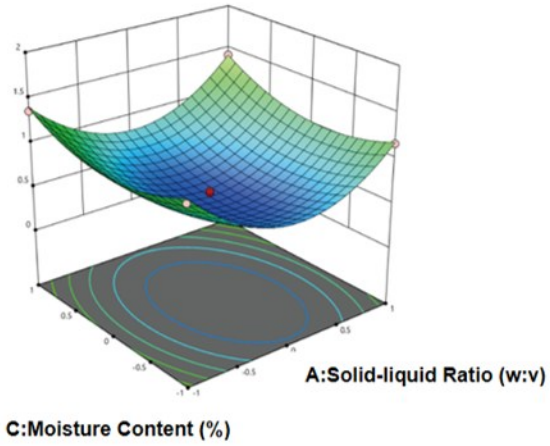

(c)

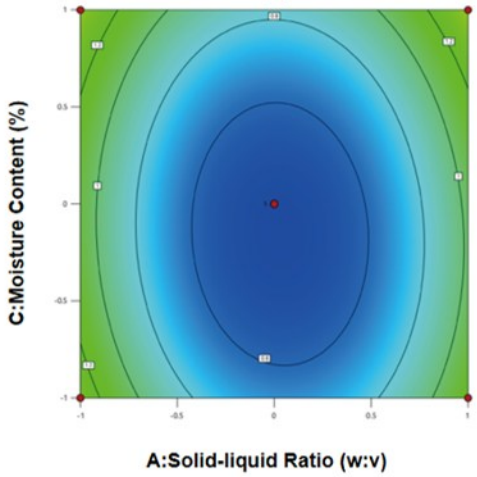

(d)

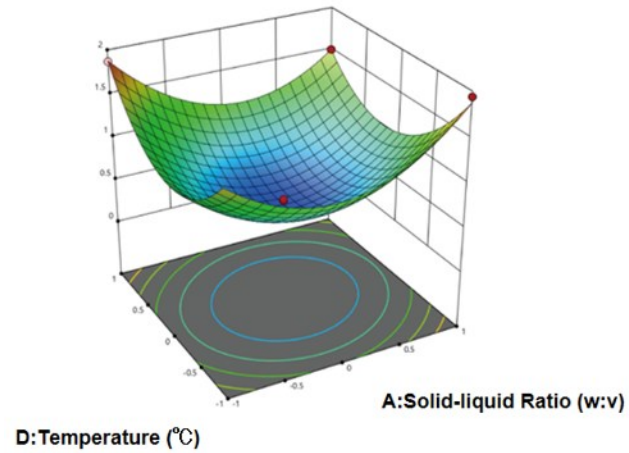
A:Solid-liquid Ratio (w:v)
D:Temperature (℃)

(e)

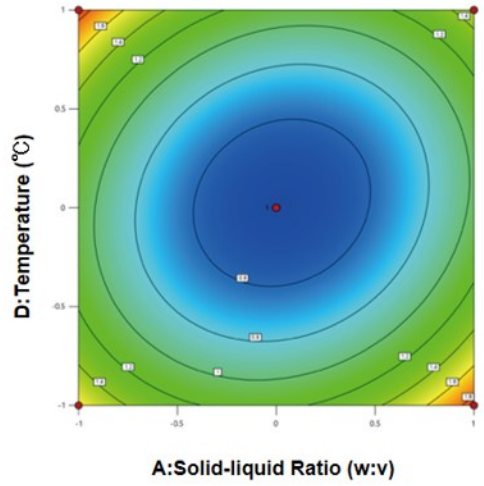
D:Temperature (℃)
A:Solid-liquid Ratio (w:v)

(f)

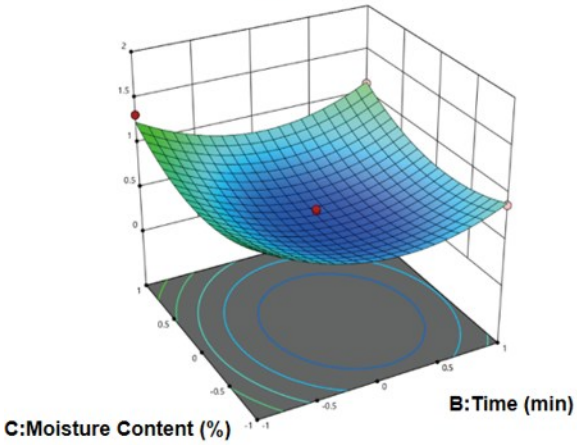
B:Time (min)
C:Moisture Content (%)

(g)

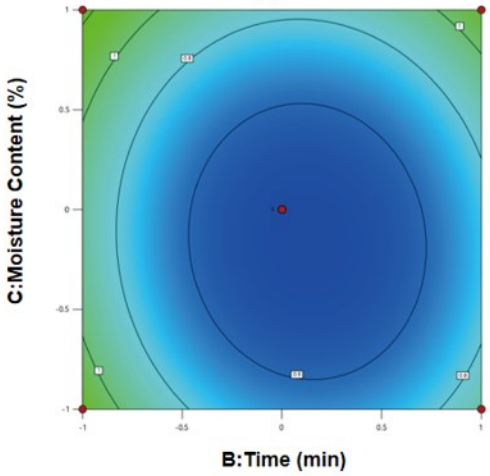
C:Moisture Content (%)
B:Time (min)

(h)

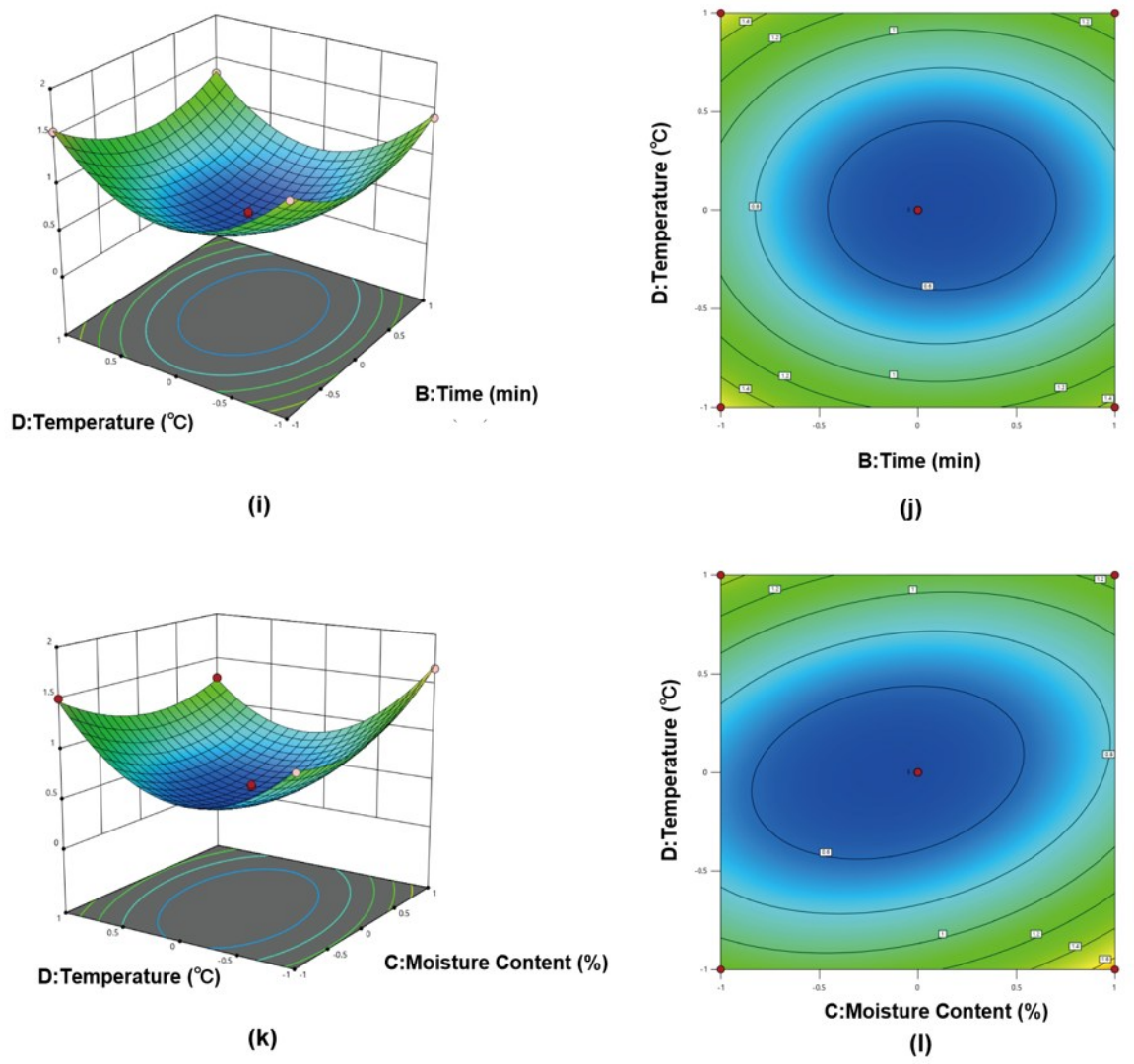

Fig. 7. (a) Response surface plot and contour plot of the ratio of feedstock to liquid and extraction time on absorbance (b); response surface plot of the ratio of feedstock to liquid and moisture content on absorbance (c) and contour plot (d); response surface plot of the ratio of feedstock to liquid and extraction temperature on absorbance (e) and contour plot (f); Extraction time and moisture content response surface plot (g) and contour plot (h); extraction time and extraction temperature response surface plot (i) and contour plot (j); moisture content and extraction temperature response surface plot (k) and contour plot (l)

Determination of extraction conditions

Response surface analysis data indicated that a ternary DES extraction process using choline chloride, ethylene glycol, and malic acid in a molar ratio of 1:3:1 was optimal for extracting *A. palmatum* dye: feed-to-liquid ratio of 1:15 (w:v), time of 112.9 min, moisture content of 86.4%, and temperature of 42.3 ℃. At this point, the absorbance was 2.91. Considering the feasibility of laboratory operations, the optimal extraction conditions were determined as follows: solid-to-liquid ratio of 1:15 (w:v), extraction time of 112 min, moisture content of 86%, and temperature of 42 ℃ After three parallel experiments, the average absorbance was 2.90, which is close to the simulated value of 2.91, indicating that the response surface optimization of the extraction conditions for *A. palmatum* dye had

reached the predicted level. The standard curve for cyanidin-3-O-glucoside quantification is provided in the Supporting Information (Fig. S1).

Study on the Stability of *Acer palmatum* Dye

The *Acer palmatum* dye solution was extracted and set aside. The optimal extraction conditions were obtained through response surface testing to examine the acid-base stability, thermal stability, and UV light stability of the dye solution, providing a reference for subsequent dyeing processes (Zhao 2015).

Effect of pH on the stability of Acer palmatum dye

Figure 8 shows digital images of *A. palmatum* dye solutions after 2 h at different pH values. The pH values of the dye solutions, from left to right, are 2, 4, 6, 8, 10, and 12. Visually, the solvent colors of the dye solutions in different acidic and alkaline environments were all red, with slight variations in shade. When the pH value was 12, the solution system was in a strongly alkaline environment, resulting in the lowest absorbance and the lightest color. As the pH value decreased gradually from 10 to 6, the solution absorbance remained stable, and the dye colors were almost identical. When the pH was 2 and 4, the solution was in a strongly acidic environment, where the absorbance increased. It reached its highest value at pH = 2, with the dye color slightly darkening. The hydroxyl, carboxyl, and amino groups of DESs in the solvent cause hydrogen bonding between the hydroxyl groups of anthocyanins and solvent molecules (Nunes *et al*. 2022). Ethylene glycol and malic acid may undergo esterification or glycosylation reactions with the hydroxyl groups of anthocyanins, forming more stable derivatives such as acylated anthocyanins, thereby reducing the dye's sensitivity to pH changes. The pH has a certain influence on the stability of *A. palmatum* dye, which is more stable under acidic conditions.

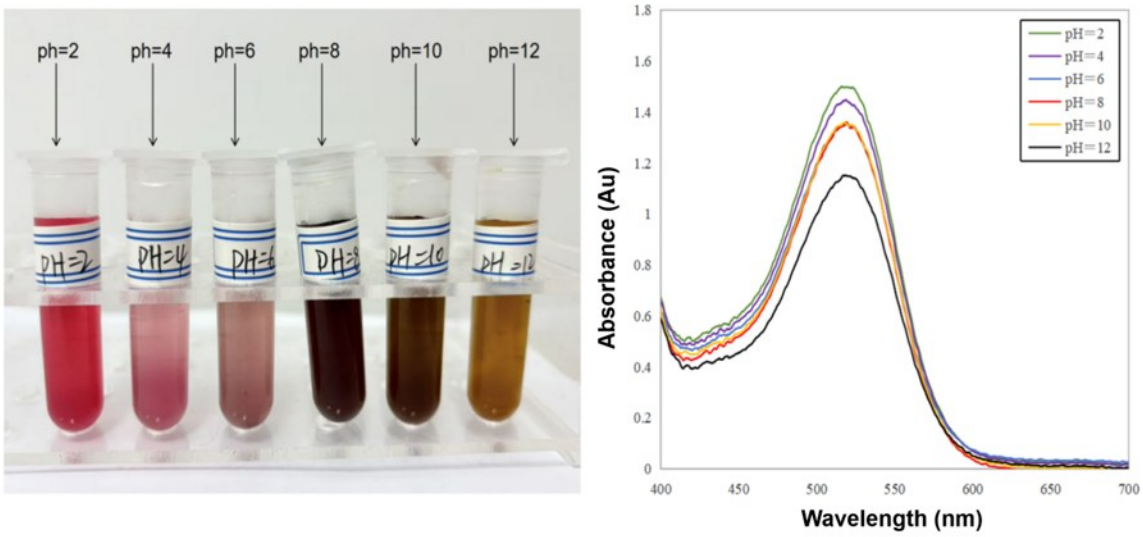

Fig. 8. Digital image showing the effect of pH on *Acer palmatum* dye

Effect of temperature on the stability of Acer palmatum dye

Figure 9 shows digital images of the *Acer palmatum* dye solution after heating in water baths at different temperatures. From left to right, the temperatures of the dye solution are 40, 50, 60, 70, and 80 °C. Visually, the color of the dye solution remained largely unchanged, and the position of the maximum absorption wavelength remained

constant. As shown in Fig. 9, temperature affected the stability of the *Acer palmatum* dye. The absorbance increased from 40 to 50 °C; above 50 °C, the absorbance decreased. It remained stable within the 60 to 80 °C range. Thus, as temperature increases, the solubility of the dye improves. The components in DESs interact with the carboxyl and hydroxyl groups of cyanidin through hydrogen bonding. This interaction reduces the movement of solute molecules, thereby reducing oxidative degradation in air (Dai *et al*. 2016), thereby significantly enhancing the dye's thermal stability.

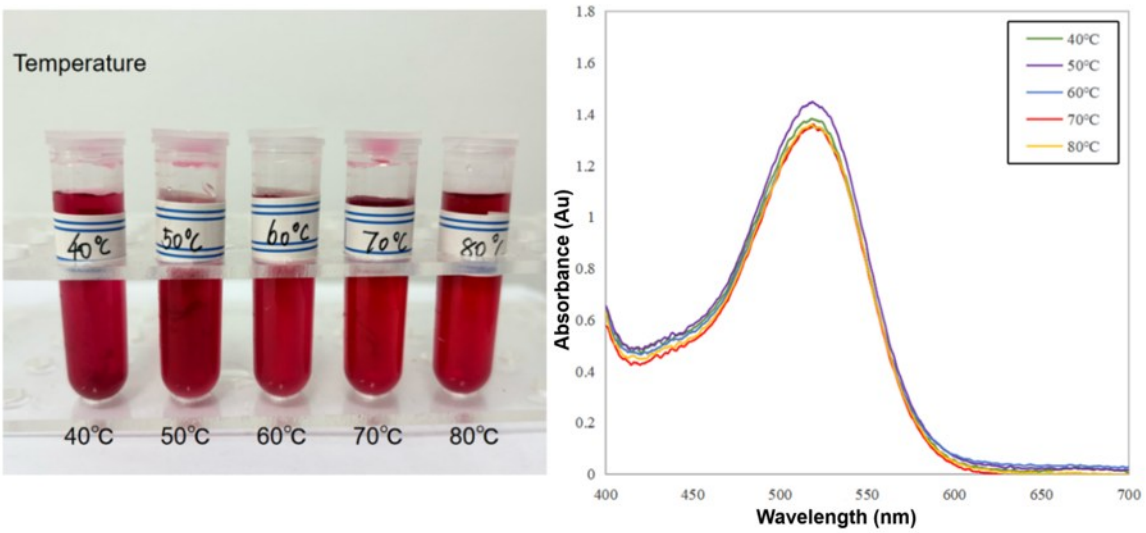

Fig. 9. Digital image showing the effect of temperature on *Acer palmatum* dye

Effect of UV irradiation on the stability of Acer palmatum dye

Figure 10 shows digital images of *Acer palmatum* dye solutions after adding pure water, DESs, 0.48 g of tea polyphenols, and 0.06 g of tea polyphenols to four groups of 20 mL *Acer palmatum* dye solutions under different UV exposure times. The line graphs represent the absorbance of dye solutions containing the same reagent after different UV exposure times. The line graph shows the peak absorbance values after different UV irradiation times. It can be observed that as the UV irradiation time was increased, the absorbance values of the *A. palmatum* dye under UV irradiation decreased, while the dye solution color remained predominantly bright red, with only variations in shade. This is attributed to the fact that the furan ring of anthocyanins is oxidized and broken, forming colorless chalcones or phenolic acids, leading to a decrease in absorbance and a lighter dye color. In Fig. 10(b), the decrease in dye absorbance within 2 to 10 h follows a linear trend. This is due to the extensive hydrogen bonding network, van der Waals, and electrostatic interactions in DESs, which inhibit the movement of photoexcited molecules (Nakhle *et al*. 2021). However, after 24 h of light exposure, the absorbance increased, possibly because water evaporation causes the viscosity of the DES solvent to rise, hindering mass transfer, leading to an increase in dye concentration and absorbance. Figures 10(c) and 10(d) show digital images of the dye's response to UV irradiation time with the addition of 0.48 g and 0.06 g of tea polyphenols, respectively. As the irradiation time was increased, the decrease in absorbance for both samples became smoother. As a natural antioxidant, tea polyphenols can scavenge free radicals and chelate metal ions, effectively preventing oxidative reactions (Sun *et al*. 2018) and reducing dye oxidation. In summary, UV light reduced the stability of *A. palmatum* dye. Therefore, UV exposure should be avoided as much as possible during the production and storage of *A. palmatum* dye.

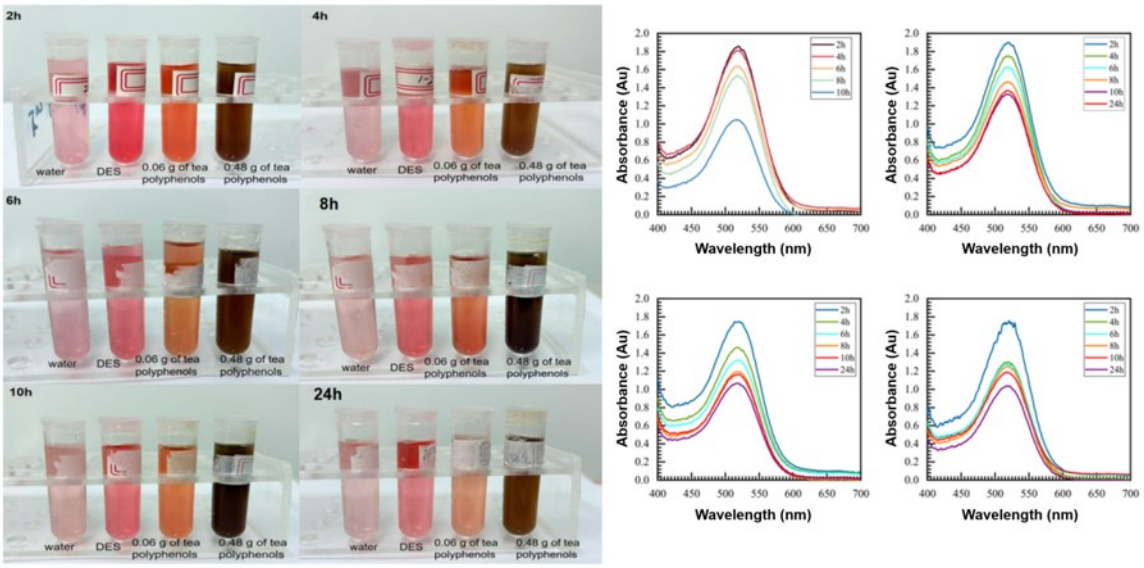

Fig.10. (a) Effect of pure water and UV irradiation time on dye stability; (b) Effect of DES and UV irradiation time on dye stability; (c) Effect of 0.48 g of tea polyphenols and UV irradiation time on dye stability; (d) Effect of 0.06 g of tea polyphenols and UV irradiation time on dye stability.

Figure 11 shows the changes in the absorbance peak of *Acer palmatum* dye with UV irradiation time after adding different reagents. After prolonged exposure to light, the absorbance of the dye added with pure water decreased significantly; the dye with added DESs showed the least change in absorbance, with the highest peak absorbance at 10 h. While the dyes with small and large amounts of tea polyphenols showed significant differences in the 2 to 5 h time window, their absorbance values became similar after 6 h, with the dye containing small amounts of tea polyphenols having a slightly higher peak absorbance than that with large amounts of tea polyphenols.

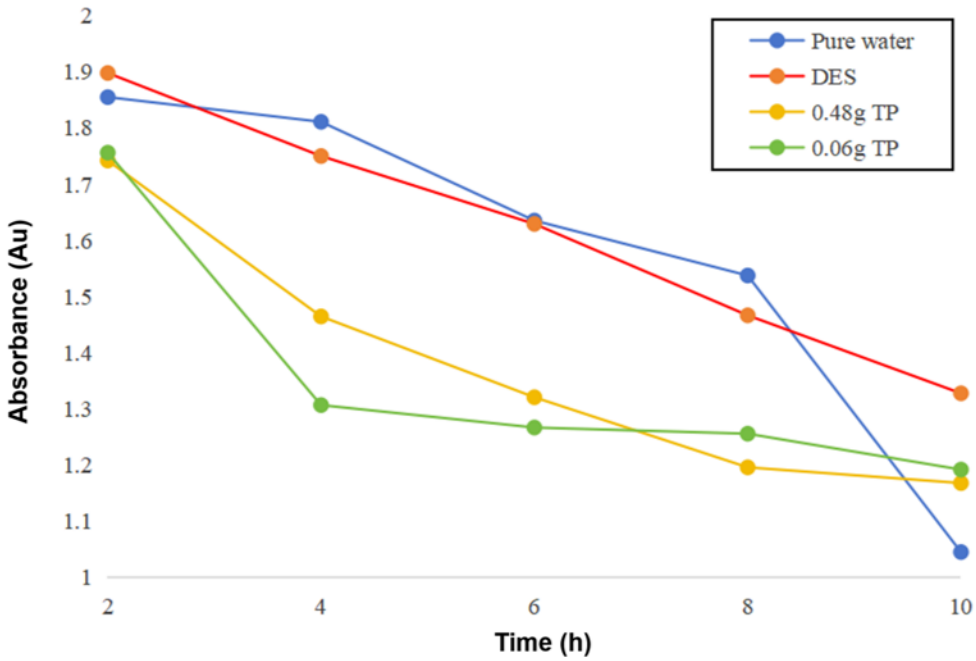

Fig.11. Effect of different reagents on the dye stability of *Acer palmatum*

As the concentration of tea polyphenols increases, the relative deficiency of dye content prevents some free phenolic hydroxyl groups from binding, leading to a decrease in absorbance. Additionally, high concentrations of tea polyphenols may alter the solution pH, affecting dye absorbance. Among the tested solvents, DESs showed the most pronounced protective effect on dye light stability under the experimental conditions examined (i.e., with DES present in the solution). However, it should be noted that in practical applications, DESs are typically removed after extraction, and therefore this protective effect may not persist in the final dye product.

In addition to optimizing extraction parameters and investigating dye stability, future research can improve the yield and stability of *A. palmatum* leaf dyes by determining suitable harvesting times. Metabolomic studies have shown that the main chromophore in maple leaves is cyanidin-3-O-glucoside (C3G), which shows obvious seasonal changes, with high contents in spring leaf expansion and autumn senescence but low levels in summer. This pattern is regulated by the ApWRKY26/ApERF4-ApMYB2-ApF3'H2 module, which promotes anthocyanin synthesis in spring and autumn while inhibiting related gene expression in summer. Harvesting leaves during spring leaf emergence or autumn color transition can therefore provide high-quality raw materials for dye extraction. Further studies may compare dye contents in leaves of different cultivars and climatic regions to identify the optimal harvesting period for maximizing bioactive chromophore retention (Zhu *et al.* 2026).

CONCLUSIONS

1. The optimal process conditions for extracting *Acer palmatum* dye using ternary deep eutectic solvent-assisted extraction were a solid-to-liquid ratio of 1:15 (w:v), a time of 112.9 min, a moisture content of 86.4%, and a temperature of 42.3 °C. Under these

conditions, the absorbance of the *A. palmatum* dye was 2.912. This was highly consistent with the model-predicted value, confirming the accuracy and reliability of the ternary deep eutectic solvent-assisted extraction process. The optimized deep eutectic solvent extraction process can be applied to actual production processes. Compared with traditional methods, this DES-based approach offers significant advantages, including reduced extraction time, improved extraction efficiency, reduced resource consumption, and enhanced production efficiency, demonstrating excellent application potential.

2. Fourier transform infrared spectroscopy analysis was performed on the *A. palmatum* dye extracted from the experiment. The dye structure contains O-H, C=O stretching vibrations of aldehyde groups, hydroxycarbonate ions (COO-), C-O and C-H groups in the phenol-aldehyde moiety, and aromatic ring skeleton. The functional groups of the main components in the red dye of *A. palmatum* were found to be consistent with those of cyanidin-3-O-glucoside, thereby confirming the chemical structure of the dye.
3. In stability studies, the results showed that solution pH, temperature, and UV light exposure all affected the stability of *A. palmatum* dye. In acidic environments (pH 2 to 6), the dye solution exhibited high absorbance and good stability. Under strongly alkaline conditions (pH 12), the compound underwent structural changes, resulting in a sharp decrease in absorbance and a fading of color. Therefore, strongly alkaline environments should be avoided for dyeing applications or storage of *A. palmatum*, with the ideal pH range for dyeing being between 2 and 6. At 40 to 50 °C, increased solvent solubility led to higher dye absorbance; above 50 °C, absorbance decreased slightly but stabilised between 60 and 80 °C. The hydrogen bond network and van der Waals forces in DESs inhibited molecular movement, reduced oxidative degradation, and enhanced thermal stability. Ultraviolet light exposure caused degradation of maple dye compounds, and the solution's absorbance and color depth were negatively correlated with exposure time. Comparisons showed that during storage of the extraction solution ternary DESs, their high viscosity hindered mass transfer and molecular movement, providing better protection for dyes than tea polyphenols, which require precise dosage control to avoid adverse effects.

ACKNOWLEDGMENTS

This work was supported by the China Qinglan Project (202002316001) and the university-enterprise collaborative education project "Household Ecological Health Application International Cooperation Joint Laboratory". College Students' Innovative Entrepreneurial Training Program "Extraction of natural plant dyes" (202410298049Z) and the Nanjing Forestry university and Collaborative Innovation Centre.

REFERENCES CITED

Abbott, A., Boothby, D., Capper, G., Davies, D., and Rasheed, R. (2004). "Deep eutectic solvents formed between choline chloride and carboxylic acids: Versatile alternatives to ionic liquids," *Journal of the American Chemical Society* 126, 9142-9147. https://doi.org/10.1021/ja048266j

An, L. J. (2012). *Cloning and Sequence Analysis for the Key Genes in Anthocyanin Biosynthesis Pathway of Acer palmatum*, Master's Thesis, Hebei Agricultural University, China.

Bişgin, A. T., Altunay, A. Ö., and Elik, A. (2025). "Ultrasound-assisted hydrophobic deep eutectic solvent-based microextraction for the spectrophotometric determination of rhodamine B," *Journal of Food Composition and Analysis* 146, article 107929. https://doi.org/10.1016/j.jfca.2025.107929

Cai, X., Li, H., Li, L., Yu, H., Chen, G., and Bao, Y. (2015). "Pigment composition and leaf color change in *Acer palmatum*," *Journal of Northeast Forestry University* 43(7), 63-67. https://doi.org/10.13759/j.cnki.dlxb.20150703.007

Cano-Lamadrid, M., Martínez-Zamora, L., Mozafari, L., Bueso, M. C., Kessler, M., and Artés-Hernández, F. (2023). "Response surface methodology to optimize the extraction of carotenoids from horticultural by-products—A systematic review," *Foods* 12, article 4456. https://doi.org/10.3390/foods12244456

Chen, Z., Ragauskas, A., and Wan, C. (2020). "Lignin extraction and upgrading using deep eutectic solvents," *Industrial Crops and Products* 147, article 112241. https://doi.org/10.1016/j.indcrop.2020.112241

Dai, Y., Rozema, E., Verpoorte, R., and Choi, Y. H. (2016). "Application of natural deep eutectic solvents to the extraction of anthocyanins from *Catharanthus roseus* with high extractability and stability," *Journal of Chromatography A* 1434, 50-56. https://doi.org/10.1016/j.chroma.2016.01.037

Diao, H., Li, L., Liang, J., Lu, C., Ding, X., and Guo, W. (2019). "Optimized extraction process and compositional analysis of bioflocculant produced by Klebsiella M1," *BioResources* 14(2), 3146-3167. https://doi.org/10.15376/biores.14.2.3146-3167

Editorial Committee of *Flora of China*. (2008). *Flora of China*, Science Press, Beijing, China.

Fu, Z. Z., Liu, J. L., and Du, J. M. (2024). "Study on dyeing process of basalt fabric with ultrafine dye," *College of Textile and Clothing* 61(6), 21-25.

Gao, Y., Fan, M., Cheng, X., Liu, X., Yang, H., Ma, W., Guo, M., and Li, L. (2024). "Deep eutectic solvent: Synthesis, classification, properties and application in macromolecular substances," *International Journal of Biological Macromolecules* 278, article 134593. https://doi.org/10.1016/j.ijbiomac.2024.134593

García, A., Rodríguez-Juan, E., Rodríguez-Gutiérrez, G., Rios, J. J., and Fernández-Bolaños, J. (2016). "Extraction of phenolic compounds from virgin olive oil by deep eutectic solvents (DESs)," *Food Chemistry* 197, 554-561. https://doi.org/10.1016/j.foodchem.2015.10.131

Jablonsky, M., Majova, V., Ondrigova, K., and Sima, J. (2019). "Preparation and characterization of physicochemical properties and application of novel ternary deep eutectic solvents," *Cellulose* 26, 3031-3045. https://doi.org/10.1007/s10570-019-02322-2

Jin, P., Wang, L., Pi, J., Yuan, T., Zhong, J., Chen, L., Huang, J., Gan, L., Lin, C., and Fan, H. (2025). "Microwave-assisted deep eutectic solvent extraction and macroporous resin purification of anthocyanins from purple-heart radish: Process optimization, structural characterization and quantitative analysis," *Food Chemistry: X* 29, article 102736. https://doi.org/10.1016/j.fochx.2025.102736

Luo, A., Yan, X., Li, L., Zhao, Z., and Tang, A. (2018). "Study on leaf color change mechanism of *Acer palmatum*," *Jiangsu Agricultural Sciences* 46(22), 118-122.

https://doi.org/10.15889/j.issn.1002-1302.2018.22.026

Nakhle, L., Kfoury, M., Mallard, I., Landy, D., and Greige-Gerges, H. (2021). "Micro-extraction of bioactive compounds using deep eutectic solvents: A review," *Environ. Chemistry Letters* 19, 3747-3759. https://doi.org/10.1007/s10311-021-01255-2

Nekkaa, A., Benaissa, A., Lalaouna, A. E. D., Mutelet, F., and Canabady-Rochelle, L. (2023). "Optimization of ultrasound-assisted deep eutectic solvent extraction of polyphenols from *Rhamnus alaternus* for their antioxidant activity," *Biomass Conversion and Biorefinery* 15, 3599-3615. https://doi.org/10.1007/s13399-023-05182-w

Nie, F., Feng, C., Ahmad, N., Tian, M., Liu, Q., Wang, W., Lin, Z., Li, C., and Zhao, C. (2023). "A new green alternative solvent for extracting echinacoside and acteoside from *Cistanche deserticola* based on ternary natural deep eutectic solvent," *Journal of Industrial and Engineering Chemistry* 118, 499-510. https://doi.org/10.1016/j.jiec.2022.11.033

Nunes, A. N., Borges, A., Matias, A. A., Bronze, M. R., and Oliveira, J. (2022). "Alternative extraction and downstream purification processes for anthocyanins," *Molecules* 27, article 368. https://doi.org/10.3390/molecules27020368

Pang, Z. S. (2000). "Overview of flavonoid research," *Beijing Agricultural Science* (05), 37-42.

Qi, Y., Liu, G., Zhang, Z., and Zhou, Z. (2023). "Optimization of green extraction process of Cinnamomum camphora fruit dye and its performance by response surface methodology," *BioResources* 18(3), 4916-4934. https://doi.org/10.15376/biores.18.3.4916-4934

Shang, X., Dou, Y., Zhang, Y., Tan, J.-N., Liu, X., and Zhang, Z. (2019). "Tailor-made natural deep eutectic solvents for green extraction of isoflavones from chickpea (*Cicer arietinum* L.) sprouts," *Industrial Crops and Products* 140, article 111724. https://doi.org/10.1016/j.indcrop.2019.111724

Sharma, S. P. (2018). "Biochar for carbon sequestration: Bioengineering for sustainable environment," in *Omics Technologies and Bio-Engineering*, Barh, D., and Azevedo, V. (eds.), Academic Press, pp. 365-385. https://doi.org/10.1016/B978-0-12-815870-8.00020-6

Sun, B., Wang, W., He, Z., Zhang, M., Kong, F., Sain, M., and Ni, Y. (2018). "Improvement of stability of tea polyphenols: A review," *Current Pharmaceutical Design* 24, 3410-3423. https://doi.org/10.2174/1381612824666180810160321

Tang, B., Zhang, H., and Row, K. H. (2015). "Application of deep eutectic solvents in the extraction and separation of target compounds from various samples," *Journal of Separation Science* 38, 1053-1064. https://doi.org/10.1002/jssc.201401347

Tian, X., and Hu, P. (2025). "Mechanism of ink and pigment detachment from palm leaf manuscripts driven by hygroexpansion," *BioResources* 20(4), 9424-9437.

Yu, D., Li, L., and Su, S. (2023). "Research progress on extracting flavonoids with deep eutectic solvents," *Science and Technology of Food Industry* 44(24), 367-375. https://doi.org/10.13386/j.issn1002-0306.2023020204

Zhao, L. Y. (2015). *Acylation Reaction of Cyanidin-3-O-glucoside with Lauric acid, its Structure Analysis and Property Evaluations*. Master's thesis, Beijing Forestry University, China.

Zhu, C., FaheemAfzalShah, Xiao, Y. L., Lu, Z., Guo, W., Xin, M., Qiu, Y. M., and Jie, R.(2026). "The ApWRKY26/ApERF4-ApMYB2 module regulates anthocyanin accumulation for the seasonal leaf color transition in *Acer palmatum*," *Horticulture Research* 13(1), article uhaf257.

Article submitted: January 22, 2026; Peer review completed: February 14, 2026; Revised version received and accepted: June 28, 2026; Published: July 10, 2026.
DOI: 10.15376/biores.21.3.7974-8000

APPENDIX

Drawing Standard Curves

Accurately weigh 5 mg of cornflower blue standard substance, dissolve it in pure water in a 50 mL volumetric flask, adjust the volume, shake well, and obtain a standard stock solution with a concentration of 0.10 mg/mL. Dilute the prepared standard stock solution in a series of concentrations: pipette 2, 3, 4, 5, 6, 7, 8, and 9 mL of the standard stock solution into 10 mL volumetric flasks. Dilute to the mark, resulting in concentrations of 0.02, 0.03, 0.04, 0.05, 0.06, and 0.07 mg/mL. Using the fixed wavelength measurement mode of the U-3900 UV spectrophotometer, 3.5 mL of the stock solution was drawn, and its maximum absorption wavelength at 514 nm was tested. A standard curve for the standard solution of chrysanthemum was plotted with the standard solution concentration (mg/mL) as the x-axis and the absorbance A as the y-axis, as shown in Fig. 8.

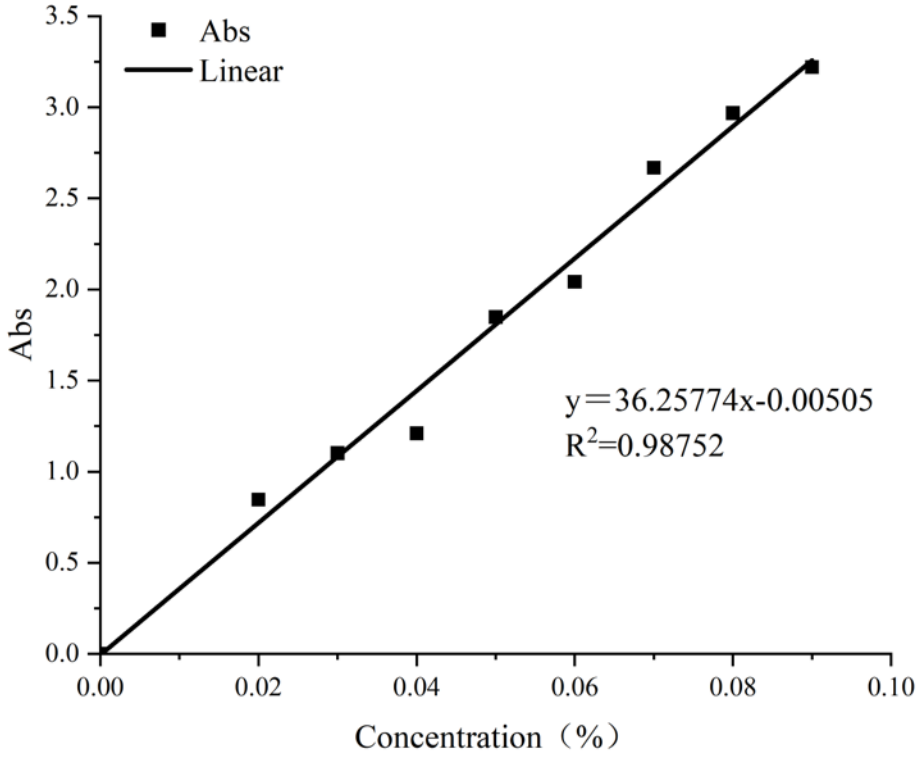

Fig. S1. Standard curve for concentration